Glass-Forming Ability and Morphological Stability of Cyclohexane and Biocyclooctene Rings Containing Disperse Red 1

John C. Mastrangelo and Shaw H. Chen*

Department of Chemical Engineering, Gavett Hall, University of Rochester, Rochester, New York 14627-0166, and Laboratory for Laser Energetics, 250 East River Road, University of Rochester, Rochester, New York 14623-1299

Thomas N. Blanton

Analytical Technology Division, Kodak Park, Bldg. 49, Eastman Kodak Company, Rochester, New York 14652-3712

Received April 13, 1995. Revised Manuscript Received August 1, 1995[⊗]

To evaluate the effects of chemical structure on the ease of vitrification, morphology, and its stability against thermally activated crystallization, disperse red 1 (DR1) was employed to synthesize di- and trisubstituted cyclohexanes and a tetrasubstituted bicyclooctene. The resultant glass-forming molecular materials were characterized with the POM, DSC, and XRD techniques across a temperature range from 25 to 225 °C. The results suggest that the DR1 derivatives of *cis*-1,2-cyclohexanedicarboxylic, 1,3,5-cyclohexane tricarboxylic, and bicyclo[2.2.2]oct-7-ene-2,3,5,6-tetracarboxylic acids yield morphologically stable glasses, with an ascending T_g from 51 to 73 and 98 °C, respectively; however, a pristine sample of the first ester was found to be crystalline and those of the other two esters completely amorphous, an indication of a stronger glass-former. In the series of disubstituted cyclohexanes, T_g was found to fall within a narrow temperature range from 45 to 52 °C, whereas a great deal of variations in morphology and its stability were observed depending on the position of substitution and stereochemistry.

Introduction

There has been a recent surge of interest in exploring organic materials for advanced optical applications in view of the versatility in molecular systems accessible through organic synthesis. Typically, desired functions of these materials can be achieved by including appropriate structural moieties. For the fabrication of optical devices, both single crystals and glasses have been attempted to avoid light scattering from grain boundaries present in polycrystalline materials. Since it is easier and less expensive to prepare glasses than single crystals, it is of inherent interest to understand glass formation by organic compounds as a basis for designing superior materials. One approach is to incorporate functional moieties as part of polymer structures that readily form glasses, leading to the so-called functional polymers. An alternative approach is to design structures of relatively low molecular weights, generally less than 1500, that possess glass-forming abilities.

Although vitrification is found to be ubiquitous in polymeric systems, it is more of an exception in low molar mass systems, especially when it comes to achieving a glass transition temperature, T_g, above the ambient. As a general observation, vitrification may occur if molecular rearrangement as a precursor to crystallization can be suppressed by a sufficiently rapid cooling rate. Our main interest lies in molecular design strategies to promote both vitrification in low molar mass materials and stability against thermally induced crystallization. The underlying concept involves two structural parameters, an excluded-volume core and a functional moiety, that are chemically bonded to each other via a flexible spacer. In a recent series of publications,[1,2] we have demonstrated the feasibility of this concept in generating glass-forming liquid crystals using cyclohexane as the excluded-volume core. We have also identified morphological stability as a hidden parameter highly relevant to practical applications,[3] which can be optimized through stereochemistry of the cyclohexane ring.[4] The present work was intended to explore disperse red 1 (DR1), a crystalline compound in its pure form, as a moiety in the design and synthesis of glass-forming optical materials. In fact, DR1 has been employed for the synthesis of side-chain polymers for potential applications to nonlinear optics[5,6] and reversible optical information storage.[7]

Using a cyclohexane ring as an excluded-volume core, we made an attempt in the present study to examine the effects of the number and position of pendant DR1 groups and the stereochemistry presented by cyclohex-

* To whom correspondence should be addressed.
⊗ Abstract published in *Advance ACS Abstracts*, September 15, 1995.

(1) Shi, H.; Chen, S. H. *Liq. Cryst.* **1994**, *17*, 413.
(2) Shi, H.; Chen, S. H. *Liq. Cryst.* **1995**, *18*, 733.
(3) Mastrangelo, J. C.; Blanton, T. N.; Chen, S. H. *Appl. Phys. Lett.* **1995**, *66*, 2212.
(4) Shi, H.; Chen, S. H. *Liq. Cryst.*, submitted.
(5) Matsumoto, S.; Kurihara, T.; Kubodera, K.; Kaino, T. *Mol. Cryst. Liq. Cryst.* **1990**, *182*, 115.
(6) Blanchard, P. M.; Mitchell, G. R. *Appl. Phys. Lett.* **1993**, *63*, 2038.
(7) Natansohn, A.; Rochon, P.; Gosselin, J.; Xie, S. *Macromolecules* **1992**, *25*, 2268.

0897-4756/95/2807-1904$09.00/0

Table 1. Proton NMR Spectral Data ($CDCl_3$, δ) of 2-[4-(4′-Nitrophenylazo)-*N*-ethyl-*N*-phenylamino]ethanol, i.e. DR1, and Its Esters with *trans*-1,2-Cyclohexanedicarboxylic, 1,3,5-Cyclohexanetricarboxylic, and Bicyclo[2.2.2]oct-7-ene-2,3,5,6-tetracarboxylic Acids

2-[4-(4′-nitrophenylazo)-*N*-ethyl-*N*-phenylamino]ethanol	1,3,5-cyclohexanetricarboxylate
1.32 ppm [t,3H,NCH_2**CH_3**]	1.27 ppm [t,9H,CH_2**CH_3**]
1.70−2.00 ppm [br,1H,**H**OCH_2CH_2]	1.30−3.00 ppm [m,9H, cyclohexane ring **H**]
3.64 ppm [m,4H,N(**CH_2**)**CH_2**]	3.53 ppm [q,6H,N**CH_2**CH_3]
3.94 ppm [br,2H,HO**CH_2**CH_2]	3.67 ppm [t,6H,N**CH_2**CH_2]
6.86 ppm [d,2H, aromatic **H** ortho to amine]	4.31 ppm [t,6H,COO**CH_2**]
7.95 ppm [m,4H, aromatic **H** ortho to N=N]	6.81 ppm [d,6H, aromatic **H** ortho to amine]
8.34 ppm [d,2H, aromatic **H** ortho to NO_2]	7.87−8.00 ppm [two d, 12H, aromatic **H** ortho to N=N]
	8.33 ppm [d, 6H, aromatic **H** ortho to NO_2]
trans-1,2-cyclohexanedicarboxylate[a]	*all-exo*-bicyclo[2.2.2]oct-7-ene-2,3,5,6-tetracarboxylate[b]
1.20−1.42 ppm [m, 10 H, overlap of two **CH_3** groups and 4 ring **H**]	1.22 ppm [t,12H,CH_2**CH_3**]
1.72−1.92 ppm [m, 2H, cyclohexane ring **H**]	3.06 ppm [s,4H,**CH** tertiary]
1.99−2.16 ppm [m,2H, cyclohexane ring **H**]	3.29 ppm [t, 2H, **CH** bridgehead]
2.57−2.72 ppm [m,2H, cyclohexane ring **H**]	3.48 ppm [q,8H,N**CH_2**CH_3]
3.56 ppm [q,4H,N**CH_2**CH_3]	3.58 ppm [t,8H,N**CH_2**CH_2]
3.68 ppm [t,4H,NCH_2**CH_2**]	4.10−4.35 ppm [m,8H,COO**CH_2**]
4.23−4.39 ppm [m,4H,COO**CH_2**]	6.38 ppm [t,2H,**CH=CH**]
6.83 ppm [d,4H, aromatic **H** ortho to amine]	6.80 ppm [d,8H, aromatic **H** ortho to amine]
7.86−8.00 ppm [two d, 8H, aromatic **H** ortho to N=N]	7.80−8.00 ppm [two d, 16H, aromatic **H** ortho to N=N]
8.35 ppm [d,4H, aromatic **H** ortho NO_2]	8.30 ppm [d,8H, aromatic **H** ortho to NO_2]

[a] Other cyclohexanedicarboxylic esters with DR1 gave similar spectral data with the exception that chemical shifts and splitting patterns in the δ 1.30−3.00 range depend on the positions of substitution and the stereochemistry of the cyclohexane ring. [b] Stereochemistry all-exo was assigned based on NMR spectral data for protons on the bicyclic ring, δ 3.06 (tertiary), 3.29 (bridgehead), and 6.38 (alkenyl) in agreement with δ 3.06, 3.31, and 6.37 reported all all-exo methyl ester of bicyclo[2.2.2]oct-7-ene-2,3,5,6-tetracarboxylic acid.[10]

ane on the glass-forming ability and morphological stability as determined by X-ray diffraction (XRD), differential scanning calorimetry (DSC), and polarized optical microscopy (POM). In addition, bicyclooctene was included as an alternative excluded-volume core to assess its effect on the ease of vitrification and morphological stability relative to cyclohexane. Because of the presence of a strong electron donor and acceptor in DR1, the trans isomer (at −N=N−) has been shown to predominate over the cis isomer.[6] Hence, the cis-trans geometric isomerism is of no concern regarding its effects on morphology and stability to be established as a part of this study.

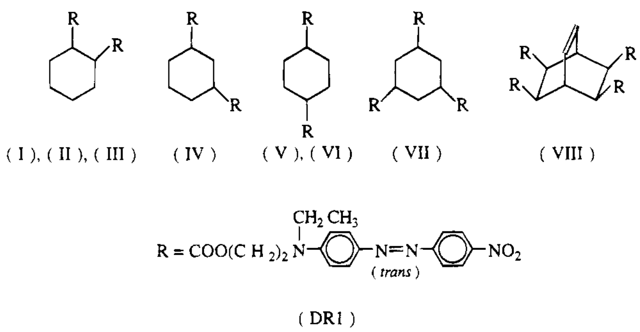

Figure 1. Chemical structures of the DR1 derivatives of cyclohexanes and bicyclooctene with stereochemical characteristics specified in Table 3 for identification of model compounds I−VIII.

Experimental Section

Reagents and Chemicals. With the exception of *cis*-1,2-cyclohexanedicarboxylic acid (98%, TCI America), all other reagents were used as received from Aldrich Chemical Co.: (±)-*trans*-1,2-cyclohexanedicarboxylic acid (95%), (±)-1,3-cyclohexanedicarboxylic acid (98%; 40% cis and 60% trans), *trans*-1,4-cyclohexanedicarboxylic acid (95%), 1,4-cyclohexanedicarboxylic acid (99%; 60% cis and 40% trans), 1,3,5-cyclohexanetricarboxylic acid (99%; 75% cis and 25% trans), triphenylphosphine (99%), diethyl azodicarboxylate (97%), disperse red 1 (i.e., 2-[4-(4′-nitrophenylazo)-*N*-ethyl-*N*-phenyl)amino]-ethanol, 30 wt % in a binder), bicyclo[2.2.2]oct-7-ene-2,3,5,6-tetracarboxylic dianhydride (98%), and anhydrous *N*,*N*-dimethylformamide (99%).

Material Synthesis. Bicyclo[2.2.2]oct-7-ene-2,3,5,6-tetracarboxylic anhydride (15 g) was stirred in 230 mL of boiling distilled water for 2 h until it was completely dissolved. Upon hot filtration, the clear solution was reduced to a solid residue via evaporation in vacuo. Bicyclo[2.2.2]oct-7-ene-2,3,5,6-tetracarboxylic acid in snow white crystals (10 g) was obtained via recrystallization from water. To isolate 2-[4-(4′-nitrophenylazo)-*N*-ethyl-*N*-phenylamino]ethanol, methylene chloride (75 mL) was added to commercially available disperse red 1 (3 g). The insoluble binder was removed via filtration, and the crude DR1 was obtained upon evaporating off the solvent in vacuo. Further purification was accomplished by recrystallization from ethanol to give dark red crystals (0.8 g). An HPLC analysis showed a purity of better than 99%. The chemical structure was found to be consistent with the proton NMR spectral data compiled in Table 1, and the DSC thermogram revealed a crystalline melting point at 165 °C with an enthalpy of melting of 88 J/g.

Model compounds synthesized for the present study are as depicted in Figure 1. The synthesis of these compounds via the Mitsunobu reaction[8] is illustrated by the following procedures. Bicyclo[2.2.2]oct-7-ene-2,3,5,6-tetracarboxylic acid (0.11 g, 0.40 mmol), 2-[4-(4′-nitrophenylazo)-*N*-ethyl-*N*-phenylamino]ethanol (0.50 g, 1.59 mmol), and triphenylphosphine (0.63 g, 2.39 mmol) were dissolved in a mixed solvent, freshly distilled tetrahydrofuran (8 mL) and anhydrous *N*,*N*-dimethylformamide (4 mL). Diethyl azodicarboxylate (0.41 mL) was then added dropwise to the solution, and the reaction was allowed to take place over a period of 4 h. Upon removing most of the solvent by evaporation in

(8) Hughes, D. L. *Organic Reactions*; Paquette, L. A., et al., Eds.; John Wiley & Sons: New York, 1992: Vol. 42, Chapter 2, pp 335−656.

Table 2. Elemental Analysis of Esters of DR1 with *trans*-1,2-Cyclohexanedicarboxylic, 1,3,5-Cyclohexanetricarboxylic, and Bicyclo[2.2.2]oct-7-ene-2,3,5,6-tetracarboxylic Acids

excluded-volume core		C %	H %	N %
trans-1,2-cyclohexanedicarboxylate[a]	calc	62.82	5.80	14.65
	obs	63.14	5.83	14.64
1,3,5-cyclohexanetricarboxylate	calc	61.95	5.47	15.21
	obs	62.26	5.46	15.08
all-exo-bicyclo[2.2.2]oct-7-ene-2,3,5,6-tetracarboxylate	calc	62.12	5.21	15.25
	obs	61.86	5.22	15.04

[a] Other cyclohexanedicarboxylic esters with DR1 showed a similar degree of agreement between observed and calculated percentages, all within 0.5% of each other.

vacuo, the crude product was collected by precipitation into ethanol (200 mL). Further purification was accomplished by liquid chromatography on silica gel (J. T. Baker, 40 μm flash chromatography packing) using methylene chloride/acetone (30:1) as the eluent followed by precipitation from a methylene chloride solution (5 mL) into methanol or *n*-hexane (100 mL), yielding red powders (0.29 g, 49%). The purity of the product was verified by HPLC analysis, and the chemical structure was elucidated with elemental analysis (see Table 2) and proton NMR spectral data as summerized in Table 1, which also contains spectral data for all cyclohexane derivatives.

Characterization Techniques. A Hitachi high-performance liquid chromatography, HPLC, system comprising an L-2000 metering pump and an L-4200 UV−vis absorbance detector equipped with an LiChrosorb column (RP-18, 10 μm) was employed to determine the number of components and purity of the intermediates and products. The purity levels of all final products were found to be better than 99% based on HPLC analysis. Chemical structures were elucidated with elemental analysis (performed by Oneida Research Services, Inc., in Whitesboro, NY), the FTIR (Nicolet 20 SXC) and proton NMR (QE-300, GE) spectroscopic techniques. Thermal transition temperatures were determined by DSC (DuPont 910 interfaced with Thermal Analyst 2100 System at a nitrogen purge of 50 cm^3/min) with morphology identified under a polarized optical microscope (Leitz Orthoplan-Pol) equipped with a hot stage (FP82, Mettler) plus a central processor (FP80, Mettler). The X-ray diffraction data were collected in reflection mode geometry using a Siemens θ/θ Bragg-Brentano diffractometer utilizing nickel-filtered Cu radiation and a Braun position sensitive detector set to measure Cu Kα radiation. This diffractometer was equipped with an Anton-Paar HTK temperature stage allowing for nonambient data collection. Samples as fine powders were placed on a sample holder comprised of a platinum ribbon. This holder was heated using resistive heating. The temperature was monitored using a thermocouple positioned beneath the sample. Samples were heated in a nitrogen atmosphere at 10 °C/min before collecting diffraction data at the specified temperatures.

Results and Discussion

The stereochemical features of cyclohexane-based systems specified in Table 3 are as provided for the starting carboxylic acids by Aldrich Chemical Co. and TCI America. The synthesis of model compounds shown in Figure 1 involves the formation of an ester linkage to cyclohexane and bicyclooctene, which is not expected to modify the stereochemical features presented by the ring structures. Nonetheless, the proton NMR spectral data provided by TCI America for diethyl esters of *cis*- and *trans*-1,2-cyclohexanedicarboxylic acids were employed to verify the stereochemical purity of the two carboxylic acids received from Aldrich Chemical Co. Specifically, the tertiary protons on the cyclohexane ring of the *cis*- and *trans*-diethyl ester showed a signal at δ 2.80 and 2.55, respectively.[9] It was found that the DR1 derivatives of the *cis*- and *trans*-1,2-cyclohexanedicarboxylic acids showed proton signals at the two chemical shifts without any stereochemical contamination, thus inspiring confidence in the stereochemical compositions specified in Table 3 for all cyclohexane-based systems. To determine the stereochemistry of the bicyclic system, NMR spectral data reported by Iordache et al.[10] for stereoisomers of bicyclo[2.2.2]oct-7-ene-2,3,5,6-tetracarboxylic methyl ester were found to be useful. Specifically, in the all-exo methyl ester, three NMR signals were identified: δ 3.06 (tertiary H), 3.31 (bridgehead H), and 6.37 (alkenyl H). As presented in Table 1, the DR1 derivative gave proton NMR signals at δ 3.06, 3.29, and 6.38 at the tertiary, bridgehead, and alkenyl position, respectively, leading to the conclusion that compound VIII as depicted in Figure 1 has an all-exo configuration.

Table 3. Thermal Transition Temperatures from DSC Second Heating Scans (at 20 °C/min Unless Noted Otherwise) with Morphology Determined by XRD and POM

model system	stereochemistry[a]	phase transition (°C)[b]	morphology of pristine sample
I	cis	g51i[c]	crystalline
II	trans	g52, 135k$_1$180k$_\infty$199i[d]	crystalline
III	50% cis, 50% trans	g49, 134k180i[e]	crystalline
IV	40% cis, 60% trans	g45, 118k136i[f]	crystalline
V	trans	g49, 102k207i[e]	crystalline
VI	60% cis, 40% trans	g47, 135k192i[e]	crystalline
VII	75% cis, 25% trans	g73i[c]	amorphous
VIII	all-exo	g98i[c]	amorphous

[a] Stereochemistry as specified by the suppliers of starting carboxylic acids with the exception of III, which was prepared as a 1:1 mixture of I and II; stereochemical purity of I and II was verified against diethyl esters of *cis*- and *trans*-1,2-cyclohexanedicarboxylic acids obtained from TCI America. [b] Symbols: g, glassy; k, crystalline; i, isotropic. [c] No crystallization observed at heating rates of 20 and 5 °C/min. [d] Glass transition at 52 °C followed by crystallization (k$_1$) and crystal modification (k$_2$) at 135 and 180 °C, respectively, and crystalline melting at 199 °C. [e] Glass transition followed by crystallization and then crystalline melting. [f] No crystallization peaks at heating rates of 20 and 10 °C/min, but a broad crystallization peak centered at 118 °C visible at 5 °C/min; however, at all three heating rates a sharp crystalline melting peak observed at 136 °C with an enthalpy of melting increasing with a decreasing heating rate.

To investigate the morphology of pristine samples, all the model systems identified in Table 3 as I−VIII were precipitated from *n*-hexane as the final purification step with the exception of III, which was prepared by blending I and II at a 1:1 ratio. The XRD patterns of pristine samples reveal a crystalline character, i.e., a multitude of sharp peaks in the $2\theta = 10-30°$ range, in

(9) Awe, C., 1995, TCI America Inc., private communications.
(10) Iordache, F.; Chiraleu, F.; Avram, M. *Rev. Roum. Chim.* **1975**, *20*, 233.

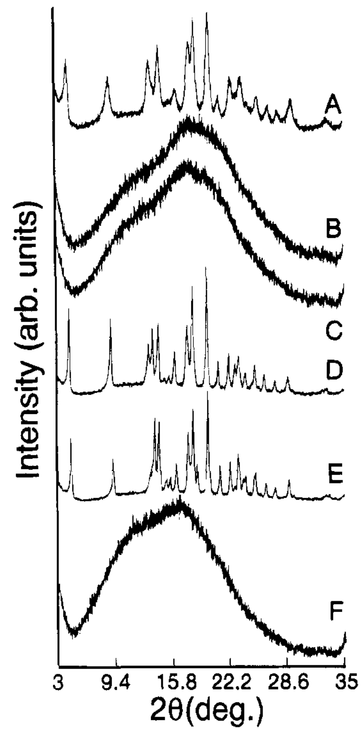

Figure 2. X-ray diffraction patterns of II, the DR1 derivative of *trans*-1,2-cyclohexanedicarboxylic acid. The pristine (i.e., freshly precipitated from n-hexane) sample was used to gather scan A. The sample was then heated to 225 °C followed by quenching at an average rate of −50 °C/min to 25 °C for gathering scan B at 25 °C, C at 75 °C, D at 150 °C, E at 185 °C, and F at 225 °C.

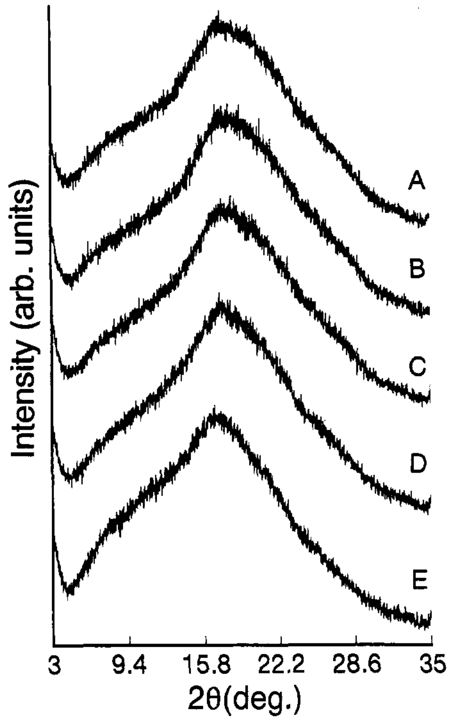

Figure 3. X-ray diffraction patterns of VIII, the DR1 derivative of bicyclo[2.2.2]oct-7-ene-2,3,5,6-tetracarboxylic acid. The pristine (i.e., freshly precipitated from n-hexane) sample was used to gather scan A. The sample was then heated to 225 °C followed by quenching to 25 °C at an average rate of −50 °C/min for gathering scan B at 25 °C, C at 75 °C, D at 125 °C, and E at 200 °C.

systems I−VI, and an amorphous character, i.e., a single broad peak in the same 2θ range, in systems VII and VIII. Representative qualitative features are as illustrated by diffraction patterns A in Figures 2 and 3 for II and VIII, respectively. Thus, it appears that systems VII and VIII are inherently strong glass-formers, in the sense that glass formation can be achieved without invoking quenching. Nevertheless, the pristine sample of I preheated to 225 °C followed by quenching to 25 °C at a rate of approximately −50 °C/min consistently showed an amorphous character, as revealed by the XRD patterns across a temperature range from 25 to 200 °C. The XRD patterns of systems II−VI pretreated the same way showed a clear evidence of thermally induced crystallization. Therefore, a preliminary idea of relative morphological stability of all the systems listed in Table 3, viz., stability against thermally induced crystallization, has emerged from comparing the XRD patterns of pristine and pretreated samples. Tentatively, morphological stability follows in decreasing order: VII, VIII > I > II, III, IV, V, VI. As to be demonstrated below, a more definitive comparison of all material systems in terms of thermal transition temperatures, morphology, and its stability can be accomplished using DSC and POM in addition to XRD.

Prior to DSC experiments, all pristine samples were heated up to 225 °C followed by cooling to −30 °C at a rate of −50 °C/min. The thermal transition temperatures reported in Table 3 were determined from the second heating scans at 20 °C/min unless noted otherwise. Let us examine the glass-forming ability and morphological stability against crystallization upon heating through T_g in terms of the position of the DR1 groups on the cyclohexane ring, stereochemical features (i.e., cis, trans and the mixture of the two), and cyclohexane vs bicyclooctene as the excluded-volume core. From the DSC thermograms of quenched glasses, systems I, VII, and VIII were found to be morphologically stable in view of the absence of crystallization peaks upon heating at 5 and 20 °C/min from 25 to 225 °C, as also verified by hot-stage POM. All these observations are in agreement with the absence of any crystalline character in the diffraction patterns of these three glasses across a temperature range from 25 to 225 °C, as illustrated by scans B−E in Figure 3 for VIII. Notice the steady increase of T_g: 51, 73, and 98 °C from I, to VII and VIII. Presumably, the number of DR1 substituent groups and the character of the excluded-volume core are important factors affecting the ease of vitrification, T_g, and morphological stability.

System IV represents an interesting case in which heating the quenched glass at a rate of 10 and 20 °C/min did not result in a crystallization peak, but a melting peak at 136 °C was observed at both heating rates, with its crystalline character identified by POM and XRD patterns. However, a broad crystallization peak centered at 118 °C followed by a sharp melting peak at 136 °C was observed as the DSC heating rate was reduced to 5 °C/min. This observation is consistent with the fact that thermally induced crystallization from an isotropic melt is a kinetic process and hence is expected to proceed to a greater extent at a lower heating rate, as validated by the observed enthalpies of melting at 136 °C: 0.8, 3.5, and 10.3 J/g at a decreasing heating rate from 20 to 10 and 5 °C/min, respectively. It is also noted that system IV is inferior to I, VII, or VIII as far as the morphological stability is

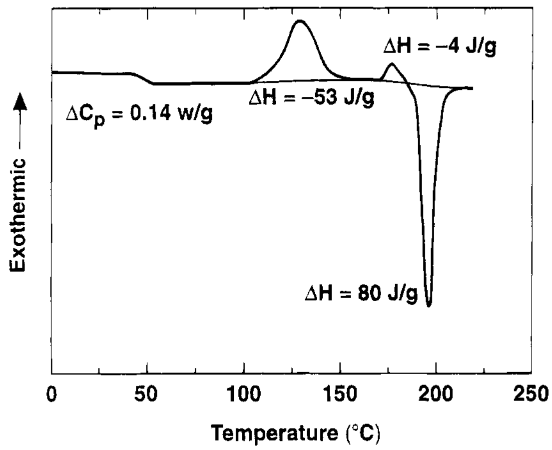

Figure 4. DSC thermogram of II, the DR1 derivative of *trans*-1,2-cyclohexanedicarboxylic acid; the sample was preheated to 225 °C followed by quenching to −30 °C at an average rate of −50 °C/min prior to gathering the presented heating scan at 20 °C/min. Note the thermal transition temperatures reported in Table 3.

concerned. The least morphologically stable systems II, III, V, and VI are characterized by crystallization peaks upon heating above T_g with crystallization temperatures as indicated in Table 3. Therefore, the combination of DSC and XRD data suggest the following decreasing order of morphological stability: VII, VIII > I > IV > II, III, V, VI.

Of the four least morphologically stable systems, III, V, and VI showed a single crystallization peak upon heating. Compound II is unique in that two exothermic peaks appeared, besides T_g and T_m, in the DSC heating scan as shown in Figure 4. To determine the nature of these two transitions, both hot-stage POM and high-temperature XRD were also employed. Although the crystalline texture was evident under POM, it was impossible to detect any phase transition between the two exothermic peaks. The XRD experiments were conducted for the sample that had been heated up to 225 °C followed by quenching to room temperature. A heating rate of 10 °C/min was then applied, and the sample was held at selected temperatures for 7 min while the diffraction data were collected. Presented in Figure 2 are the XRD patterns as a function of temperature for II. Note that crystalline characters are clearly shown in the XRD patterns and that the XRD patterns taken at 150 and 185 °C differ from each other in minor details. These observations coupled with the fact that the first exothermic peak at 135 °C is characterized by a much greater enthalpy of transition than the second exothermic peak at 180 °C, 53 vs 4 J/g, suggest that the former is likely to be crystallization from an isotropic melt and the latter some form of crystalline modification.

To validate the direct comparison between XRD and DSC data gathered inevitably under different experimental conditions, an additional DSC experiment was conducted in which a quenched sample of compound II was heated to 150 °C at 20 °C/min and kept there for 10 min before continuing with the same heating rate up to 225 °C. The crystalline modification was observed at 180 °C with an enthalpy of transition of 4 J/g, a value identical to that observed in a continuous DSC heating scan all the way from 25 to 225 °C as reported in Figure 4. Thus, no crystalline modification had occurred during the 10 min holding time at 150 °C, suggesting that the minor difference in the XRD patterns between D and E in Figure 2, is indeed a consequence of crystalline modification. In other words, XRD patterns D and E in Figure 2 should not be dismissed as identical to each other.

In short, it is concluded that in the disubstituted cyclohexane systems, T_g falls within a narrow temperature range from 45 to 52 °C; however, there seems to be a great deal of variation in morphology and its stability depending on the position of substitution and the stereochemical features on the cyclohexane ring. Conversely, in the three morphologically stable glasses derived from *cis*-1,2-cyclohexanedicarboxylic, 1,3,5-cyclohexanetricarboxylic (75% cis and 25% trans), and *all-exo*-bicyclo[2.2.2]oct-7-ene-2,3,5,6-tetracarboxylic acids, there is a steady elevation of T_g from 51 to 73 and 98 °C. These results provide a foundation for the optimization of glass transition temperature, morphology, and its stability for practical applications.

Acknowledgment. We thank Professor A. S. Kende of the Department of Chemistry, University of Rochester, for assistance with organic synthesis, Professor A. Natansohn of the Department of Chemistry, Queen's University in Canada for her insight into the geometric isomerism of DR1, and Mr. K. L. Marshall and Dr. Ansgar Schmid of the Laboratory for Laser Energetics for technical assistance and helpful discussions. We would like to express our gratitude to Kaiser Electronics for financial support of this research and National Science Foundation for an engineering research equipment grant, CTS-9411604. The work reported here was also supported in part by a NEDO project sponsored by the Ministry of International Trade and Industry of Japan. In addition, our liquid crystal materials research was supported in part by the US Department of Energy, Division of Inertial Confinement Fusion under Cooperative Agreement No. DE-FC03-92SF19460 with the University of Rochester.

CM950174T